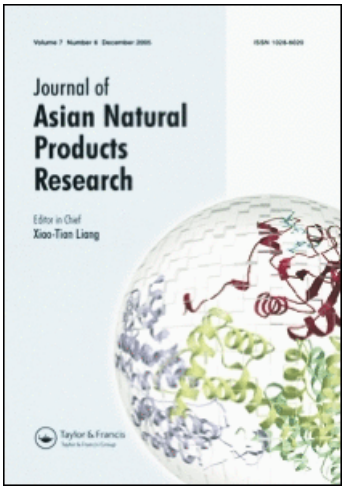

Journal of Asian Natural Products Research
Publication details, including instructions for authors and subscription information:
http://www.informaworld.com/smpp/title~content=t713454007

SAHA and curcumin combinations co-enhance histone acetylation in human cancer cells but operate antagonistically in exerting cytotoxic effects

Jin-Yan Zhao[a]; Na Lu[a]; Zheng Yan[a]; Nan Wang[a]
[a] Institute of Materia Medica, Chinese Academy of Medical Sciences & Peking Union Medical College, Beijing, China

Online publication date: 20 May 2010

To cite this Article Zhao, Jin-Yan , Lu, Na , Yan, Zheng and Wang, Nan(2010) 'SAHA and curcumin combinations co-enhance histone acetylation in human cancer cells but operate antagonistically in exerting cytotoxic effects', Journal of Asian Natural Products Research, 12: 5, 335 — 348
To link to this Article: DOI: 10.1080/10286021003730348
URL: http://dx.doi.org/10.1080/10286021003730348

Journal of Asian Natural Products Research
Vol. 12, No. 5, May 2010, 335–348

ORIGINAL ARTICLE

SAHA and curcumin combinations co-enhance histone acetylation in human cancer cells but operate antagonistically in exerting cytotoxic effects

Jin-Yan Zhao, Na Lu, Zheng Yan and Nan Wang*

Institute of Materia Medica, Chinese Academy of Medical Sciences & Peking Union Medical College, Beijing 100050, China

(*Received 16 December 2009; final version received 25 February 2010*)

Suberoylanilide hydroxamic acid (**1**), as well as other histone deacetylase (HDAC) inhibitors, are promising, targeted anticancer agents. Curcumin (**2**), a possible antitumor agent, exhibits a HDAC inhibiting effect but with a different mechanism, and was proposed to synergize with other drugs, including HDAC inhibitors. The present study was undertaken to evaluate the possible inhibitory effects of **1** and **2** combinations on the growth of nine human cancer cell lines. Drug combinations resulted in an antagonistic cytotoxic effect, as characterized by the Loewe additivity model, observed in all the cell lines. On the other hand, histone hyperacetylation was synergistically or at least additively induced by **1** and **2** combinations, in four cell lines tested. Despite the enhanced histone acetylation, **1** plus **2** produced a significant antagonism in the induced activation of downstream $p21^{CIP/WAF1}$ expression. Concomitantly, induced reactive oxygen species (ROS) production was antagonistically diminished in combinations especially at low concentration of **2**. We conclude that **1** and **2** exert an antagonistic cytotoxicity on a variety of cancer cell lines, and suggest that mechanisms mediating their antagonism lie at levels of $p21^{CIP/WAF1}$ expression and ROS production, rather than at histone acetylation.

Keywords: cancer; histone deacetylase inhibitors; SAHA; curcumin; drug interaction

1. Introduction

Levels of histone acetylation in chromatin are modulated by counteracting histone deacetylases (HDAC) and histone acetyltransferases (HAT), affecting chromatin structural organization, and regulating gene expression and DNA-related cellular events. HDAC inhibitors affect a subset of gene expression patterns by modifying core histone acetylation. They have also been shown to exert antitumor effects in preclinical studies and clinical trials, and represent a new class of targeted anticancer agents [1]. Suberoylanilide hydroxamic acid (SAHA, **1**; Figure 1) was the first agent of this category approved for clinical treatment of cutaneous T-cell lymphoma [2].

HDAC inhibitors seem to be quite suited for combination treatment with existing chemotherapy regimens [3]. For instance, **1** is synergistic in anticancer activity with a number of chemotherapeutic agents, including tyrosine kinase inhibitors such as imatinib, topoisomerase II inhibitors, hormone antagonists, and differentiating agents such as retinoic acid.

Curcumin (Cur, **2**; Figure 1), a natural polyphenol used in ancient Asian medicine, exhibits a variety of pharmacological

*Corresponding author. Email: wangnan@imm.ac.cn

ISSN 1028-6020 print/ISSN 1477-2213 online

DOI: 10.1080/10286021003730348
http://www.informaworld.com

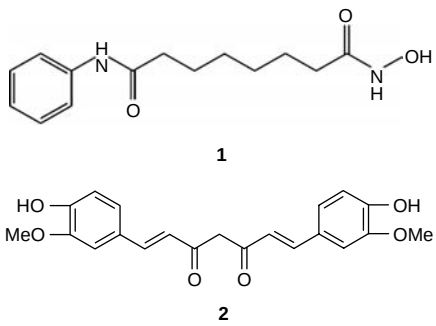

Figure 1. Chemical structures of SAHA (**1**) and Cur (**2**).

effects such as anti-inflammatory, antioxidant, wound healing, and anticancer activities. Compound **2** also shows synergistic effects in combination with some cytotoxic drugs [4] or agents. Multiple targets have been proposed for its chemopreventive and chemotherapeutic action toward cancer. Recent results [5,6] demonstrated that **2** is a HAT inhibitor that induced histone hypoacetylation in cells derived from various origins. It has also been evidenced that **2** promotes acetylation of histones H3 and H4 of tumor cells and inhibits the expression of class I HDACs (HDAC1, HDAC3, and HDAC8) [7], rather than direct inhibition of HDAC activity [6], suggesting that **2** is a novel member of HDAC inhibitors. Curcumin (**2**)-induced histone acetylation has usually been observed at lower concentrations (below 20 μM) while acetylation inhibition was generally observed at higher concentrations.

Since **2** has a different mechanism of HDAC inhibition as classic HDAC inhibitors, one might speculate that combining **2** with a 'true' HDAC inhibitor would provide a potentiating effect on cancer cell death by enhanced histone modification. Indeed, evidence has been provided [8] that combinations of low concentrations of **2** and a typical HDAC inhibitor trichostatin A (TSA) increased histone acetylation, and showed increased cytotoxicity for HL-60 cells, with a diminished generation of reactive oxygen species (ROS). In the present study, we have investigated the effects of combined **2** and **1** on cytotoxicity in a wide variety of human cancer cell lines derived from solid tumors, and on the synergism or antagonism in enhancing histone acetylation and induced downstream $p21^{CIP/WAF1}$ expression, and ROS production. The results are entirely contrary to the expectations.

2. Materials and methods

2.1 Drugs and chemicals

SAHA (**1**) was synthesized by Prof. Song Wu at our Institute. Cur (analytical grade) was obtained from Beijing Chemical Reagents Co. (Beijing, China). SAHA (**1**) and Cur (**2**) were dissolved in MSO at the desired concentrations and diluted into cell culture media at a maximal concentration below 0.1%, which was also present in the corresponding controls. Dichlorodihydrofluorescein diacetate (DCFH-DA) was obtained from Sigma-Aldrich (St Louis, MO, USA). 3-(4,5-Dimethylthiazol-2-yl)-2,5-diphenyltetrazolium bromide (MTT) and RPMI-1640 medium were obtained from Invitrogen (Carlsbad, CA, USA). All other chemicals were of analytical grade.

2.2 Cell culture

The human cancer cell lines, A549 and NCI-H460 (lung cancer), HeLa (cervical cancer), BGC-803 (stomach cancer), PC-3M (prostate cancer), HCT-8 (colon cancer), HepG2 and H7402 (hepatic cancer), and Ketr3 (renal cancer) were maintained in RPMI-1640 medium, supplemented with 10% heat-inactivated fetal bovine serum (Sijiqing Biomaterial, Hangzhou, China) and 100 units/ml of both penicillin and streptomycin, in a humidified 5% CO_2/air atmosphere at 37°C. All of the above cells were from the American Type Culture Collection (ATCC) or Cell Culture Center of Institute of Basic Medical Sciences, Chinese Academy of Medical Sciences.

2.3 Cytotoxicity assay

An MTT assay was used to determine the cytotoxicity of drugs. Briefly, logarithmic cells were plated in the 96-well plates at concentrations of 1200–1500/100 μl per well. Drugs at different concentrations were added with four replicates after 24 h. The cells were further incubated at 37°C for 72 h, the medium was then aspirated, and 100 μl MTT of 0.5 mg/ml in a medium was added. After 4 h incubation, the medium was aspirated again and 150 μl DMSO was added to solubilize the formazan crystals. Absorbance of the converted dye was measured at 570 nm with background subtraction at 655 nm. The dose-response curves were fitted with SigmaPlot and IC_{50} values were determined.

2.4 Western blotting

To determine histone acetylation status, cultured cells (BGC-803, HeLa, HepG2, and A549) were harvested and histones were isolated by acid extraction. Purified histones were electrophoresed on a 12% SDS-PAGE gel and transferred by electroblotting onto a nitrocellulose membrane. The blots were stained with Ponceau S as a normalization of the loading difference. Acetylated histone H3 (Ac-H3) was detected with a rabbit polyclonal anti-human acetylated H3 antibody (Upstate Biotechnology, Lake Placid, NY, USA, No. 06-599), diluted 1:5000 in 5% non-fat dried milk powder in phosphate buffered saline (PBS), containing 0.05% Tween-20. Immunoblots were incubated with a secondary antibody labeled with HRP (Zhongshan Goldenbridge Biotechnology, Beijing, China, No. ZB-2301) and visualized by chemiluminescent detection according to the manufacturer's instruction (Vigorous Biotechnology, Beijing, China). Quantitation of histone acetylation levels was done by densitometric analysis with QuantiScan software, according to the following equation: fold of acetylation induction = (density of Ac-H3 band in treated cells/density of Ac-H3 band in untreated cells)/(density of Ponceau S-stained band in treated cells/density of Ponceau S-stained band in untreated cells).

2.5 RNA extraction and RT-PCR

Total RNA was isolated from cells (BGC-803, HeLa, HepG2, and A549) with RNA extraction reagent RNAvzol (Vigorous Biotechnology), according to the instructions, and $p21^{CIP/WAF1}$ mRNA expression was detected by semi-quantitative RT-PCR. Five micrograms of total RNA were reverse-transcribed into cDNA with MMLV reverse transcriptase (Dingguo Biotechnology, Beijing, China) and random primers in a 20 μl volume at 42°C for 50 min. PCR primers for $p21^{CIP/WAF1}$ were 5′-GCCTGCCGCCGCCTCTTC-3′ as the forward primer and 5′-GCCGCCTGCCTCCTCCCAACTC-3′ as the reverse primer with a predicted product of 235 bp. GAPDH was used as an internal control in the same PCR reaction with forward primer 5′-GGCAAATTCCATGGCACCGTCAAG-3′ and reverse primer 5′-GCAATGCCAGCCCCAGCGTCAAA-3′ and a predicted product of 745 bp. The conditions for PCR consisted of initial denaturation (95°C/3 min), 21–22 cycles of denaturation (95°C/10 s), annealing (64°C/10 s), extension (72°C/15 s), and a final extension (72°C/7 min). After reaction, PCR products were separated on a 2% TAE agarose gel containing ethidium bromide, visualized, and recorded under UV light. Relative $p21^{CIP/WAF1}$ mRNA expression in treated cells was measured by densitometry analysis with QuantiScan software, according to the following equation: fold of $p21^{CIP/WAF1}$ induction = (density of $p21^{CIP/WAF1}$ band in treated cells/density of $p21^{CIP/WAF1}$ band in untreated cells)/(density of GAPDH band in treated cells/density of GAPDH band in untreated cells).

2.6 Measurement of intracellular ROS production

Intracellular ROS generation was detected by a DCFH-DA fluorescent probe and flow cytometry. In brief, drug-treated culture cells were washed, trypsinized, and collected, suspended in a serum-free medium (1×10^6/ml) containing 5 μM (for BGC-803 and HepG2) or 10 μM (for HeLa and A549) DCFH-DA and incubated for 30 min at 37°C in a final volume of 1 ml. Cells were washed, resuspended in PBS on ice, and analyzed using a FACS instrument (Coulter ELITEESP, Beckman Coulter Co., Brea, CA, USA) at 488 nm excitation and 530 nm emission, respectively. In the presence of ROS, DCFH is oxidized to the highly fluorescent 2′,7′-dichlorofluorescein. The fluorescent intensity is proportional to the amount of intracellular ROS generated.

2.7 Drug combination and data analysis

In addition to the untreated cell controls and cells treated with each drug alone, fixed concentrations of **1** were combined with varying concentrations of **2** and applied to the cells simultaneously. In the cytotoxicity assay, 0.33 and 1 μM of **1** were combined with **2** at various concentrations of up to 100 μM. In the evaluation of histone acetylation, $p21^{CIP/WAF1}$ expression and ROS generation, 1 μM of **1** was combined with low concentrations of **2** at 0.1–10 μM.

Drug combination data was analyzed using the widely accepted Loewe additivity (LA) drug interaction model. The LA theory is described by the following equation: $d_A/D_A + d_B/D_B = 1$, where d_A and d_B are the concentrations of the drugs A and B in the combination which exert a certain effect and D_A and D_B are the iso-effective concentrations of the drugs A and B when used alone. If the experimental product of this equation (Loewe combination index, LCI) is equal to 1, the data are considered additive; indices of <1 or >1 indicate synergy or antagonism, respectively.

For the assessment of combined effects on cytotoxicity, the CombiTool program (version 2.001) was used to quantify differences between observed effects and those predicted by the LA equation and to calculate LCI [9]. Single-drug dose-response curves were first fitted using a logistic model with SigmaPlot. Parameters for each drug were then entered into the logistic function of CombiTool to generate the expected effect of drug combinations, based on an additive Loewe interaction. 3D plots depicting the differences between the experimental (observed) and predicted data were generated. The method of Chou and Talalay [10], based on the median-effect principle of the mass-action law, was also utilized to assess the type of drug interaction and combination index (CI) was calculated by CompuSyn (version 1.0.1).

To evaluate the combined effects on histone acetylation, $p21^{CIP/WAF1}$ expression and ROS generation, it was assumed that the dose-response curves generally approximate to linearity in the low dose/low effect region used in those experiments. The effect summation method was used to calculate the predicted effect of a zero-interactive combination. In LA theory, it is reasonable to expect that, in the absence of interaction, the effect of a combination will be the sum of the effects of its constituents in the low dose/low effect region [11]. The experimental (observed) and predicted data were compared to determine the additivity, synergy, or antagonism.

All data are presented as mean ± standard deviation (SD). Statistical analysis was carried out by two-way ANOVA and the Student t-test with $p < 0.05$ representing significance.

3. Results

3.1 Cytotoxicity of SAHA, Cur, and the combination thereof

SAHA (**1**) and Cur (**2**) caused cell growth inhibition of all cell lines tested. SAHA (**1**) inhibited the cells more potently with IC_{50}

Table 1. Cytotoxicity profile of Cur and SAHA in a panel of human cancer cell lines.

Cell	Tumor type	Cur, IC_{50} (μM)	SAHA, IC_{50} (μM)
HCT-8	Colorectal carcinoma	15.98 ± 2.556 (4)	1.50 ± 0.408 (4)
BGC-803	Gastric carcinoma	5.16 ± 0.884 (3)	0.89 ± 0.243 (3)
HeLa	Cervical carcinoma	18.10 ± 2.318 (3)	1.54 ± 0.362 (3)
Ketr3	Renal carcinoma	25.42 ± 0.677 (3)	1.69 ± 0.21 (3)
PC-3M	Prostate adenocarcinoma	19.54 ± 0.889 (3)	0.81 ± 0.318 (3)
H7402	Hepatic carcinoma	24.22 ± 8.136 (5)	2.21 ± 0.748 (3)
HepG2	Hepatic carcinoma	7.06 ± 0.298 (5)	0.49 ± 0.222 (5)
A549	NSCLC	11.17 ± 7.593 (3)	0.54 ± 0.146 (3)
NCI-H460	NSCLC	16.08 ± 0.007 (2)	2.94 ± 0.284 (2)

Note: Mean IC_{50} values and SD were calculated from several independent MTT assays (number of replicates shown in parentheses). NSCLC, non-small cell lung cancer.

values at micromolar level, while **2** generally had higher IC_{50} values ranging at 5–30 μM level, as shown in Table 1.

When the cells were treated simultaneously with **1** and **2**, using low concentrations of **2** (below 10 μM), it was generally observed (Figure 2(a)) that cell growth inhibition was lower than the effect of the same concentration of **1** alone. This is a clear indication for drug antagonism based on the LA model [11]. When 3D response plots were constructed and the expected effects of drug combinations compared with that of the experimental data (Figure 2(b)), statistically relevant antagonism was observed in all cell lines at different combinations. LCI calculated as depicted in Figure 3(a) further supported antagonism for the **1** and **2** combination on cytotoxicity. Averaged LCI ranged from 1.37 to 3.55 for the nine cell lines tested. CI, calculated by the method of Chou and Talalay, averaged from 1.20 to 3.24 for the cell lines, also suggested a general antagonism for the **1** and **2** combination, although the specific pattern of CI distribution (shown in Figure 3(b)) at each combination differs from that of LCI, suggesting a tendency of synergy at higher **2** concentrations.

3.2 Enhanced histone acetylation by SAHA, Cur, and combinations thereof

As **2** acts as both an HDAC inhibitor and HAT inhibitor, we were interested to see whether the HAT inhibiting effect would diminish the HDAC inhibition action of **1**, especially at low concentrations, which might account for their antagonism in cytotoxicity. Four cell lines (BGC-803, HeLa, HepG2, and A549) were treated with **1** at 1 μM, **2** at 0.1, 1, and 10 μM for 22 h, and histone H3 acetylation was detected. Whereas **1** significantly augmented the histone H3 acetylation to about two- to three-fold of the untreated control, **2** induced a marginal increase of H3 acetylation, with statistical significance only in HepG2 and A549 cells at 1 μM concentration (Figure 4). Dose-dependency of acetylation enhancement by **2** was slightly more prominent in BGC-803 and HepG2 cells. When the cells were treated with combined **1** and **2** at above concentrations for 22 h, histone H3 acetylation was further enhanced by **2** in a dose-dependent manner in all four cell lines. The enhanced acetylation levels were compared with the expected effects of drug combinations. Significantly higher acetylation was evidenced in A549 and HeLa cells ($p < 0.05$ by two-way ANOVA), indicating a synergy in histone acetylation. Acetylation levels similar to the predicted effects were observed in BGC-803 and HepG2 cells ($p < 0.05$ by two-way ANOVA), suggesting a general additivity for combined **1** and **2**.

The effect summation method was used with the assumption that the dose-response curves were within linear ranges in the low

dose/low effect region. Cur (**2**) barely induced histone acetylation in any of the four cell lines. The response curves were flat and not expected to rise any further as histone deacetylation would appear at higher concentrations [5,6]. Instead, **1** was a strong inducer of histone acetylation. It is reasonable to assume that the concentration of **1** (1 μM) was within approximate linear range under the hypothesis of a simple additive Loewe interaction, as the combined responses did show linearity upon increasing concentrations of **2**. Actually, the levels of induced

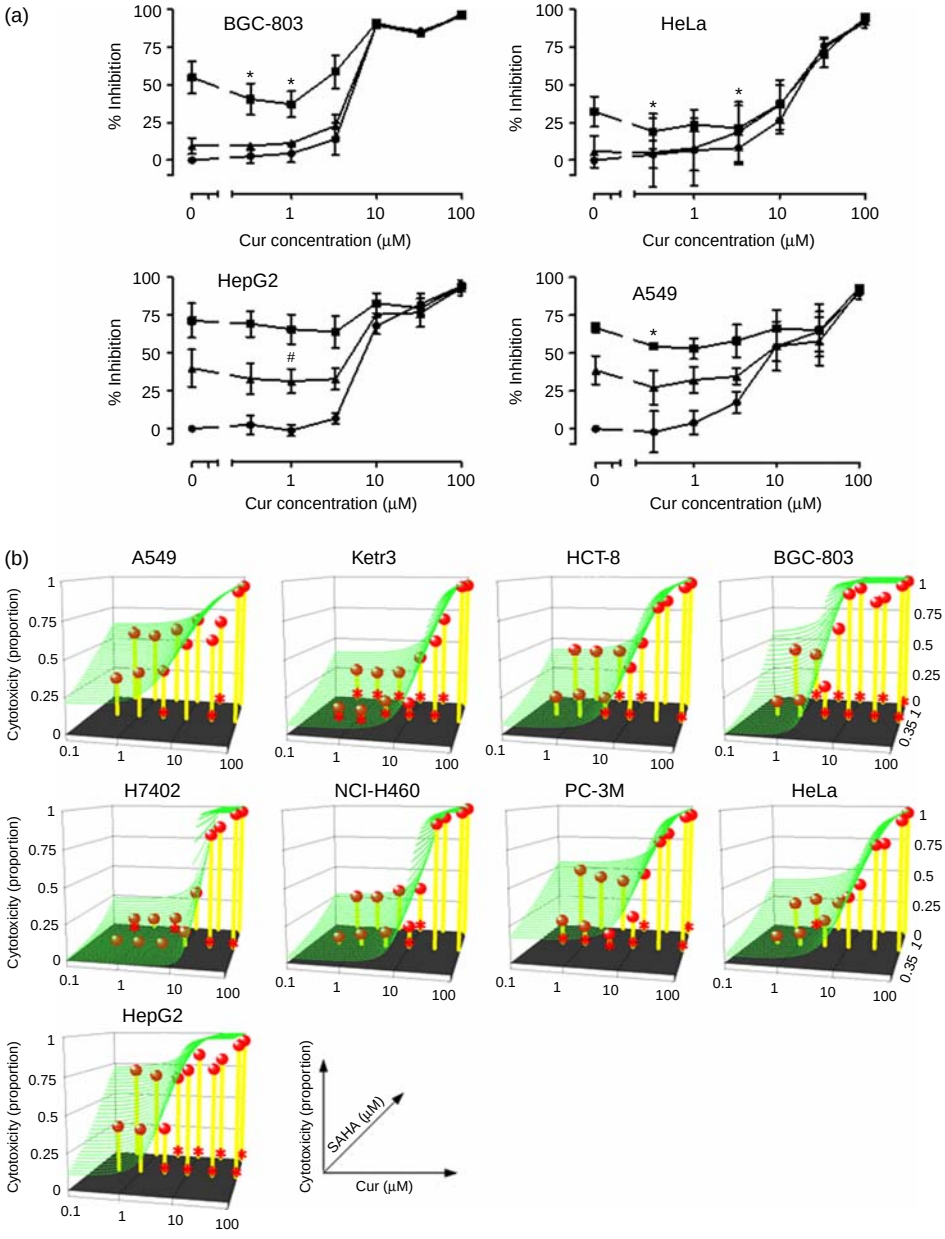

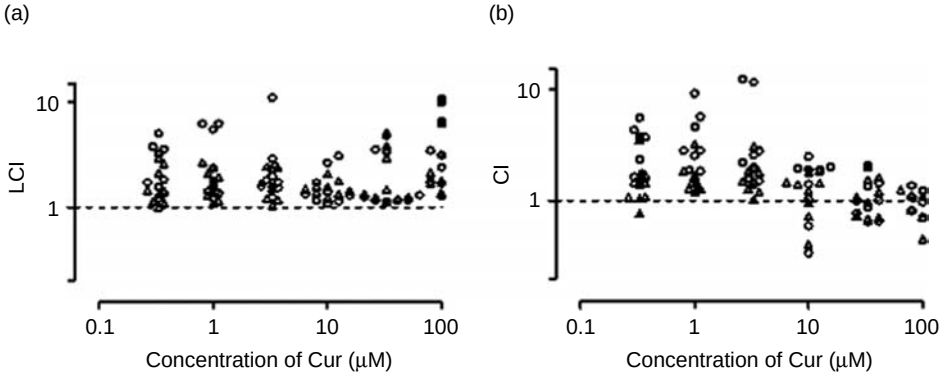

Figure 3. Drug interaction indices of combined SAHA–Cur on cytotoxicity. (a) Individual LCI calculated with CombiTool and (b) Chou's CI calculated with CompuSyn, upon every combination of Cur and SAHA at 0.33 (circles) or 1 μM (triangles) for the cytotoxicity assay in all nine cell lines, were plotted as a function of concentrations of Cur. If the value is less than 1, the combination is considered synergistic; if greater than 1, antagonistic; if equal to 1, additive.

acetylation were usually approaching saturation at 1 μM of **1**, as reported and as previously observed by us in different cells. In this situation, where response curves for **1** were in the 'high effect' region, not within linear range but rather than in a region of concaved downward lines, greater quantities of **1** alone were needed to get the effects compared to that calculated from linear ranges. In the left-hand part of the LA equation, $d_{Cur}/D_{Cur} + d_{SAHA}/D_{SAHA}$, an increase in D_{SAHA} will make the actual results much lower than calculated from linear ranges. Hence, it was appropriate for us to evaluate the synergy (but not antagonism), with the predicted effects by calculating their summation. It would be safe to say that combined **1** and **2** produced a synergy on inducing histone acetylation in two of the four cell lines, and at least additivity in the other two cell lines, if not undervalued for synergy.

3.3 Antagonism of combined SAHA and Cur on inducing p21$^{CIP/WAF1}$ expression

The cell-cycle inhibitor p21$^{CIP/WAF1}$ mediates cell growth inhibition and is also a common target gene subject to modulation by HDAC inhibitors. We investigated whether p21$^{CIP/WAF1}$ levels increased at enhanced histone acetylation when cells were treated with **1** and **2** combinations. A semi-quantitative RT-PCR procedure was used for the determination of

Figure 2. Interaction between SAHA and Cur on the growth inhibition of human cancer cell lines. Cells were treated with the drugs for 72 h and then cell viability was assessed using the MTT assay as described in Section 2. (a) Curves of growth-inhibitory effects of Cur, in the absence (circle) and presence of SAHA at concentrations of 0.33 μM (triangle) or 1 μM (square), are shown for four of the cell lines. Each data point is the mean and SD of three (for BGC-803, HeLa, and A549) or five independent experiments (for HepG2). Data are expressed as percent inhibition of cell proliferation vs. control cells. Statistical significances of the difference between the reduced effects of combinations and SAHA alone are indicated by the asterisk ($*p < 0.05$). (b) The 3D zero-interaction response surfaces (the Loewe additive model), shown in green, are derived from single-agent experiments. The observed combination responses (as a proportion) are the mean of three to five independent experiments for all cell lines except for NCI-H460 (two experiments), shown as red spheres. Most of the experimental combinatorial effects are below the zero-interaction response surface, and considered antagonistic. The asterisk indicates a significant difference between the observed response and the corresponding value on the surface ($*p < 0.05$ by t-test) (color online).

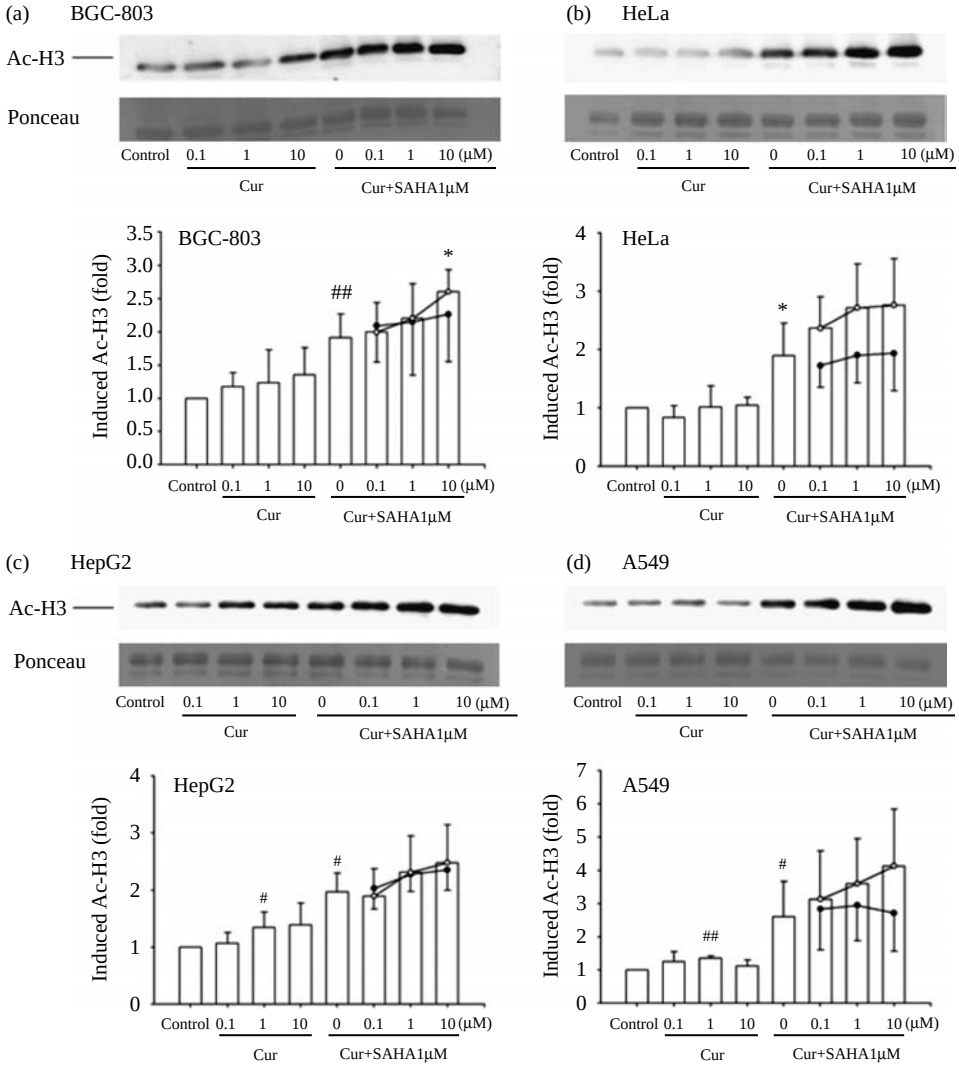

Figure 4. Effect of SAHA–Cur combined treatment on histone H3 hyperacetylation. BGC-803, HeLa, HepG2, and A549 cells were treated with 1 μM SAHA, or 0.1, 1, and 10 μM Cur, or combinations of both, for 22 h and then Ac-H3 was detected by Western blotting. For normalization purposes, the blots were stained with Ponceau S. Bars in the graphs represent means and SD of four independent experiments. A typical Western blot is shown in each upper panel. Single-drug-induced acetylation was compared with no-treatment control ($^{\#}p < 0.05$, $^{\#\#}p < 0.01$ by *t*-test), and that of combination induced with 1 μM SAHA treatment alone ($^{*}p < 0.05$ by *t*-test). Combined effects (line with open circles) were also compared with corresponding expected effects calculated by the summation method (line with filled circles) using two-way ANOVA.

$p21^{CIP/WAF1}$, which was previously validated by real-time PCR. As shown in Figure 5, $p21^{CIP/WAF1}$ mRNA was moderately induced by **2** in a dose-dependent manner, most significantly at 10 μM after 22 h treatment, with a maximal induction of 1.5- to 2-fold. SAHA (**1**) significantly induced $p21^{CIP/WAF1}$ mRNA expression to a greater extent than **2**, maximum to 2.5- to 5.5-fold, in a dose-dependent manner.

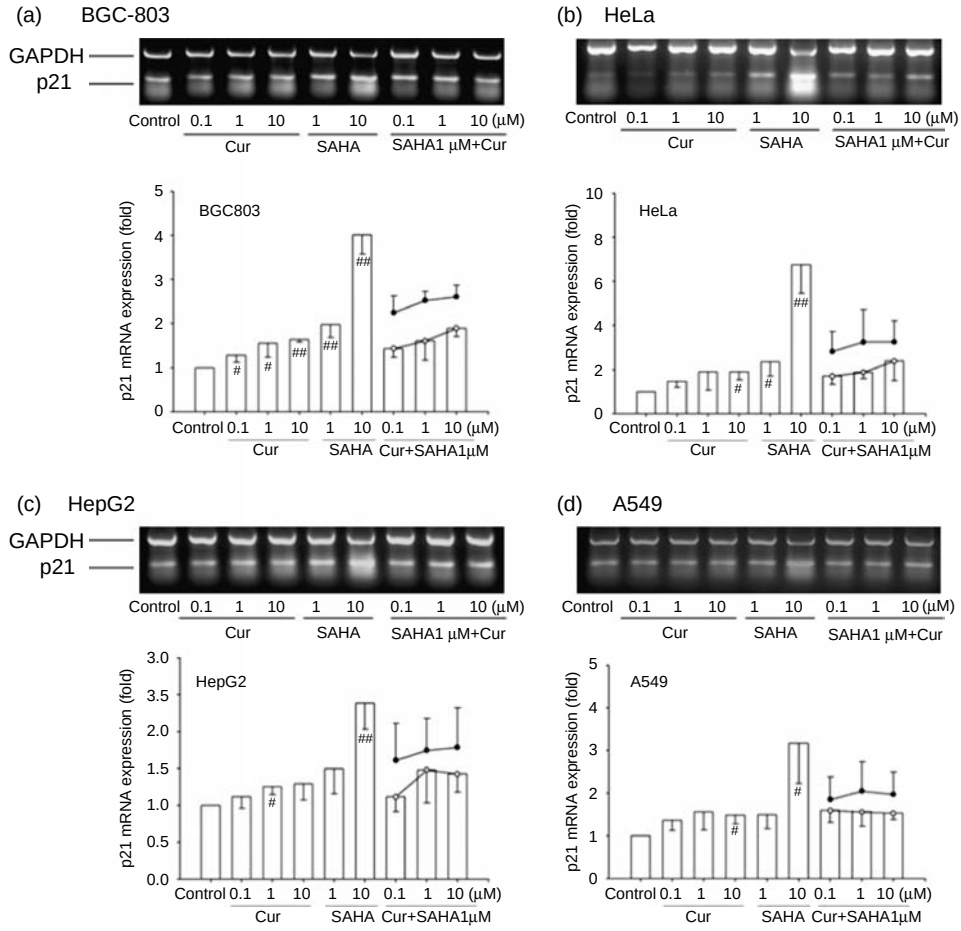

Figure 5. Effect of SAHA–Cur combined treatment on $p21^{CIP/WAF1}$ mRNA expression. (a) BGC-803, (b) HeLa, (c) HepG2, and (d) A549 cells were treated with 1 and 10 μM SAHA, or 0.1, 1, and 10 μM Cur, or combinations of both, as indicated for 22 h, and then $p21^{CIP/WAF1}$ mRNA expression was determined by semi-quantitative RT-PCR with p21 specific primers and GAPDH as the internal control. Typical results of gel analysis of semi-quantitative RT-PCR are shown in each of the upper panels. Bars in the graphs represent means and SD of three independent experiments. Drug-induced gene expression was compared with no-treatment control ($^{\#}p < 0.05$, $^{\#\#}p < 0.01$ by *t*-test). Combined effects (line with open circles) were also compared with corresponding expected effects calculated by the summation method (line with filled circles) using two-way ANOVA.

When **2** (0.1, 1, and 10 μM) was combined with **1** (1 μM), inducible $p21^{CIP/WAF1}$ mRNA expression was not further enhanced, if not decreased, as compared to **1** alone. The combined effects were significantly lower than the expected effects calculated by summation rule in all the four cell lines tested ($p < 0.05$ by two-way ANOVA), indicating an antagonistic effect of the combined **1** and **2** on the induction of $p21^{CIP/WAF1}$ mRNA expression, at the concentrations used.

The dose responses of induced $p21^{CIP/WAF1}$ mRNA expression by **1** and **2** at combined low concentrations were low as compared to that of **1** at 10 μM. The predicted, summed effects were also well below the maximum effects of **1**

alone. The effect summation would be appropriate for calculating the predicted effects. Since the effects of combined 1 μM of **1** with **2** at various concentrations were almost the same as, if not less than, that of 1 μM of **1** alone (i.e. roughly $d_{SAHA} = D_{SAHA}$ in the left-hand part of the LA equation: $d_{Cur}/D_{Cur} + d_{SAHA}/D_{SAHA}$), we should obtain values for all the products >1, indicating antagonism.

3.4 Antagonism of combined SAHA and Cur on inducing ROS generation

As expected, both **1** and **2** enhanced the intracellular ROS production in a dose-dependent manner (Figure 6). While in combination with 1 μM of **1**, **2** (at 0.1 μM) reduced the ROS level significantly in the four cell lines tested as compared to **1** alone, indicating antagonism at this combination, according to LA theory. When the combined effects were compared with the expected effects calculated with the summation method, a markedly diminished generation of ROS was observed in BGC-803, HeLa, and A549 cells (by two-way ANOVA, $p < 0.01$), which further supported the general antagonism of **1** and **2** activities in these cell lines. Although in HepG2 cells, two-way ANOVA did not identify a significant difference between the combined effects and the expected effects ($p > 0.05$), the effect of combination at 10 μM of **2** was significantly lower than the expected effects ($p < 0.05$ in a *t*-test), suggesting an antagonism at this combination in HepG2. We are quite confident about the result of antagonism of combined **1** with **2** at 0.1 μM, as it was not based on any assumptions. We would cautiously suggest that antagonism existed for combined **1** with **2** at higher concentrations for those cells if the assumption of linearity was not overvalued.

4. Discussion

The search for combinations of drugs is a valuable route for finding better treatment of cancer. In addition to its potential clinical value, measurement of drug interactions is an important first step in understanding the possible mechanisms responsible for the interaction, even for a single drug.

In the present work, we used fixed concentrations of **1** combined with varying concentrations of **2** to observe their interactions, a valid and frequently used experimental design [11]. The combined data on cytotoxicity were readily analyzed parametrically by software based on the LA interaction model, indicating antagonistic action between **1** and **2**. Slight discrepancies were seen only at higher concentrations of **2** with Chou's CI model. It has been proposed that Chou's CI method is more appropriate in analyzing the fixed-ratio designed data. Decreased cytotoxicity was usually observed at lower concentrations of **2** combined with **1**, in contrast to an earlier report [8] where combinations of low **2** and TSA showed a more significant cytotoxicity in HL-60 cells.

For a typical drug combination experiment, the dose-response curve for each single drug should first be obtained, then the drugs were mixed at designed ratios, and responses were observed. For the cytotoxicity assay, it was done in this way. However, owing to cytotoxicity and the dual action of **2** on histone acetylation and ROS generation [8], it was not possible to evaluate the full range of dose-response curves for **1**, and especially for **2**, of the single and combined effects on histone acetylation, $p21^{CIP/WAF1}$ expression, and ROS generation. Fortunately, full dose-response curves are not always required for drug interaction determination, as discussed by Berenbaum [11]. Since we were focusing on the effects of **2** at lower concentrations with more HDAC inhibiting activity rather than HAT inhibiting activity, as proposed [8], only low

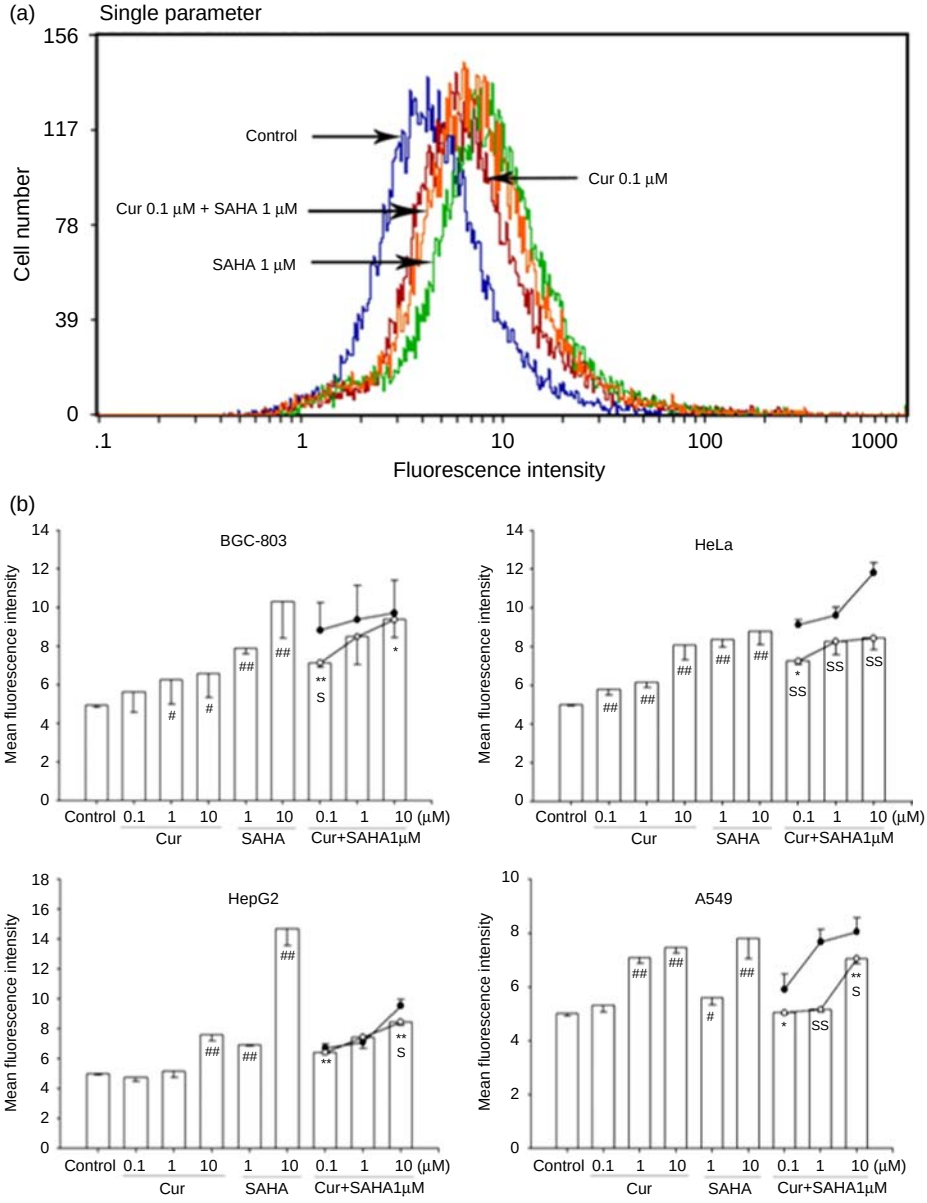

Figure 6. Effect of SAHA–Cur combinations on intracellular ROS production. BGC-803, HeLa, HepG2, and A549 cells were treated with 1 and 10 μM SAHA, or 0.1, 1, and 10 μM Cur, or combinations of both, as indicated for 22 h, and then intracellular ROS generation was determined by the fluorescent probe DCFH-DA with flow cytometry. (a) Typical histograms obtained for HeLa cells were shown. (b) Bars in the graphs represent means and SD of three independent experiments. Single-drug-induced ROS was compared with no-treatment control ($^{\#}p < 0.05$, $^{\#\#}p < 0.01$ by *t*-test), and that of combination compared with 1 μM SAHA treatment alone ($*p < 0.05$, $**p < 0.01$ by *t*-test). Combined effects (line with open circles) were also compared with corresponding expected effects calculated by the summation method (line with filled circles) using two-way ANOVA or *t*-test ($^{\$}p < 0.05$, $^{\$\$}p < 0.01$).

concentrations (up to 10 μM) of **2** and **1** at 1 μM were combined for these experiments. The combined data can be analyzed non-parametrically with the LA method, usually under the assumption that the dose-response curves were within linear ranges in the low dose/low effect region.

HDAC inhibitors cause accumulation of acetylated histones in tumor and in normal cells with subsequent transcriptional activation of a defined set of genes through chromatin remodeling. Histone H3 and H4 acetylation in peripheral blood mononuclear cells has been the most frequently used molecular biomarker in clinical trials. Although acquired resistance to **1** was correlated with loss of histone acetylation [12], hyperacetylated histones are not sufficient to cause growth inhibition in all cell types [13], and histone acetylation did not predict clinical responses as well. In our experiment, **1** in combination with low concentrations of **2** enhanced the histone acetylation, probably through different HDAC inhibiting mechanisms. This is in line with the result [8] that combinations of low concentrations of **2** and TSA could increase histone acetylation in HL-60 cells. But the enhanced histone acetylation did not lead to a combined increase in cytotoxicity, conforming to an earlier model [13] that growth inhibition caused by HDAC inhibitors may be the culmination of histone hyperacetylation acting in concert with other growth regulatory pathways.

$p21^{CIP/WAF1}$ is transcriptionally activated by HDAC inhibitors, and therefore associated with histone hyperacetylation. In fact, increased $p21^{CIP/WAF1}$ levels contribute to the anti-proliferative activity of HDAC inhibitors [14]. Cur (**2**) also induces overexpression of $p21^{CIP/WAF1}$ in various cancer cells, explaining, at least in part, its cytotoxicity [15]. But it is currently not known if this induction of $p21^{CIP/WAF1}$ is correlated with the epigenetic modifying property of **2**. Still, there is also a controversy on the exact role of $p21^{CIP/WAF1}$ in cytotoxicity of HDAC inhibitors, due to the ability of $p21^{CIP/WAF1}$ to block apoptosis. Drug combinations which attenuate the $p21^{CIP/WAF1}$ expression induced by HDAC inhibitors usually produce synergistic anticancer effects [16]. Whereas, in **2** combinations, elevated $p21^{CIP/WAF1}$ expression has been associated with and contributes to an enhanced cytotoxicity [17], antagonism of **1** and **2** in cytotoxicity in the current study is associated with antagonistic action on $p21^{CIP/WAF1}$ induction. Even at the low concentrations of **2**, which did not cause cell growth inhibition, reduced cytotoxicity was observed for **1** accompanying a reduction in $p21^{CIP/WAF1}$ expression, proposing a positive role of $p21^{CIP/WAF1}$ induction in cytotoxicity of **1** and its combinations. The changes of $p21^{CIP/WAF1}$ induction are reversed compared to those of induced histone acetylation in response to combined drugs. This is in agreement with recently published results [18] that changes in histone acetylation are not correlated with downstream $p21^{CIP/WAF1}$ gene activation following exposure to HDAC inhibitors.

SAHA (**1**), as well as other HDAC inhibitors, causes an increase in ROS, which plays an important role in inducing cytotoxicity and accounts for their selectivity on cancer cells [19]. Cur (**2**) is a ROS inducer in cancer cells [20] and its cytotoxicity is correlated with the levels of induced ROS [21]. It also acts as an antioxidant with ROS-inhibiting activities, and antagonizes the cytotoxicity induced by other agents through ROS inhibition [22,23]. Reduced cytotoxicity of combined **1** and **2** is associated with diminished ROS generation in our present work, in keeping with the results [22,23] of combined antagonism associating with ROS inhibition, as well as the results [24,25] that combined synergy of HDAC inhibitors and other agents was associated with augment in ROS production. It is puzzling that a previous paper [8] indicated enhanced

cytotoxicity of combined TSA and **2** associated with and attributed to diminished ROS generations in HL-60 cells. Discrepancy may exist between cell lines, where TSA alone showed no effect on ROS generation, **2** in low and high concentrations diminished or promoted it, respectively, in HL-60 cells [8], which is different from what we observed in other cell lines.

In summary, by reliably defining additive, synergistic, and antagonistic interactions, we demonstrate that simultaneous treatment of **1** and **2** exhibits an antagonistic cytotoxic effect toward a series of nine cell lines from solid tumors. The combination treatment produced enhanced (synergistic or at least additive) histone acetylation tested in four of those cell lines, without augment in subsequent $p21^{CIP/WAF1}$ expression. Instead, induction of both $p21^{CIP/WAF1}$ expression and ROS generation was antagonistically diminished, especially at combined low concentrations of **2**, although each of the two drugs enhanced them alone. The experimental evidence from this study suggests that overall histone acetylation is neither an indication for cytotoxic response, nor a predictor of gene expression in response to HDAC inhibitors alone or in combination. The findings also indicate that, in contrast to previous results [16], combined antagonism in $p21^{CIP/WAF1}$ gene activation does not always produce a synergy in cytotoxicity, and imply that both induced $p21^{CIP/WAF1}$ gene expression and enhanced ROS generation in response to HDAC inhibitors act as mediators rather than interrupters for their cytotoxic effects.

Acknowledgements

The authors thank Prof. Song Wu and colleagues in our Institute for the synthesis of **1**, Dr Jürgen Sühnel of the Fritz Lipman Institute (Jena, Germany) for providing CombiTool software, and Dr Ting-Chao Chou of the Memorial Sloan-Kettering Cancer Center (New York, USA) for providing CompuSyn software. We are grateful to Prof. Paul Tempst of the Memorial Sloan-Kettering Cancer Center (New York, USA) for critical reading and helpful discussions of the manuscript. This paper was supported by the funding of the National Critical Drug Innovation Project (2009ZX09301-003-9-1) from the Chinese Ministry of Health.

References

[1] J.E. Bolden, M.J. Peart, and R.W. Johnstone, *Nat. Rev. Drug Discov.* **5**, 769 (2006).
[2] P.A. Marks, *Oncogene* **26**, 1351 (2007).
[3] M. Bots and R.W. Johnstone, *Clin. Cancer Res.* **15**, 3970 (2009).
[4] S.E. Chuang, P.Y. Yeh, Y.S. Lu, G.M. Lai, C.M. Liao, M. Gao, and A.L. Cheng, *Biochem. Pharmacol.* **63**, 1709 (2002).
[5] K. Balasubramanyam, R.A. Varier, M. Altaf, V. Swaminathan, N.B. Siddappa, U. Ranga, and T.K. Kundu, *J. Biol. Chem.* **279**, 51163 (2004).
[6] J. Kang, J. Chen, Y. Shi, J. Jia, and Y. Zhang, *Biochem. Pharmacol.* **69**, 1205 (2005).
[7] H.L. Liu, Y. Chen, G.H. Cui, and J.F. Zhou, *Acta Pharmacol. Sin.* **26**, 603 (2005).
[8] J. Chen, H. Bai, C. Wang, and J. Kang, *Pharmazie* **61**, 710 (2006).
[9] V. Dressler, G. Müller, and J. Sühnel, *Comput. Biomed. Res.* **32**, 145 (1999).
[10] T.C. Chou and P. Talalay, *Adv. Enzyme Regul.* **22**, 27 (1984).
[11] M.C. Berenbaum, *Pharmacol. Rev.* **41**, 93 (1989).
[12] K.J. Dedes, I. Dedes, P. Imesch, A.O. von Bueren, D. Fink, and A. Fedier, *Anticancer Drugs* **20**, 321 (2009).
[13] H. Brinkmann, A.L. Dahler, C. Popa, M.M. Serewko, P.G. Parsons, B.G. Gabrielli, A.J. Burgess, and N.A. Saunders, *J. Biol. Chem.* **276**, 22491 (2001).
[14] S.Y. Archer, S. Meng, A. Shei, and R.A. Hodin, *Proc. Natl Acad. Sci. USA* **95**, 6791 (1998).
[15] R.K. Srivastava, Q. Chen, I. Siddiqui, K. Sarva, and S. Shankar, *Cell Cycle* **6**, 2953 (2007).
[16] R.R. Rosato, J.A. Almenara, C. Yu, and S. Grant, *Mol. Pharmacol.* **65**, 571 (2004).
[17] T.C. Hour, J. Chen, C.Y. Huang, J.Y. Guan, S.H. Lu, and Y.S. Pu, *Prostate* **51**, 211 (2002).

[18] D.J. Ellis, Z.K. Lawman, and K. Bonham, *Biochem. Biophys. Res. Commun.* **367**, 656 (2008).
[19] J.S. Ungerstedt, Y. Sowa, W.S. Xu, Y. Shao, M. Dokmanovic, G. Perez, L. Ngo, A. Holmgren, X. Jiang, and P.A. Marks, *Proc. Natl Acad. Sci. USA* **102**, 673 (2005).
[20] J. Fang, J. Lu, and A. Holmgren, *J. Biol. Chem.* **280**, 25284 (2005).
[21] N. Hail, Jr., *Free Radic. Biol. Med.* **44**, 1382 (2008).
[22] S. Somasundaram, N.A. Edmund, D.T. Moore, G.W. Small, Y.Y. Shi, and R.Z. Orlowski, *Cancer Res.* **62**, 3868 (2002).
[23] J. Cao, Y. Liu, L. Jia, L.P. Jiang, C.Y. Geng, X.F. Yao, Y. Kong, B.N. Jiang, and L.F. Zhong, *J. Agric. Food Chem.* **56**, 12059 (2008).
[24] M. Rahmani, E. Reese, Y. Dai, C. Bauer, S.G. Payne, P. Dent, S. Spiegel, and S. Grant, *Cancer Res.* **65**, 2422 (2005).
[25] S.K. Seo, H.O. Jin, H.C. Lee, S.H. Woo, E.S. Kim, D.H. Yoo, S.J. Lee, S. An, C.H. Rhee, S.I. Hong, T.B. Choe, and I.C. Park, *Mol. Pharmacol.* **73**, 1005 (2008).